Characterization of multilayer TiO_2 /ZnO nanostructured thin films using Raman spectroscopy

L. G. BOUSIAKOU[a,b,*], T. GANETSOS[b], R. QINDEEL[a], W. A. FAROOQ[a], A. FATEHMULLA[a], SYED MANSOOR ALI[a]
[a]*Department of Physics and Astronomy, College of Science, King Saud University, Riyadh, Saudi Arabia*
[b]*Department of Automation Engineering, Piraeus University of Applied Sciences, Egaleo Athens, 12244, Greece*

The aim of this paper is to characterize TiO_2/ ZnO multilayer thin films using Raman spectroscopy. The TiO2/ZnO films were prepared using the sol-gel spin coating method. Additionally the surface morphology and crystal structure of thin films were characterized by means of profilometry. The profilometer results showed that the surfaces of the samples are not uniform. The thickness of the sample was identified in the μm range. Raman spectroscopy revealed a sharp and strong peak at 436.9 cm^{-1} due to ZnO. The observed peak is assigned as the optical phonon E2 mode which is a characteristic Raman-active peak for the wurtzite hexagonal phase of ZnO. The TiO_2/ZnO substrate exhibited many peaks. The existence of the 436.9 cm^{-1} peak in the TiO_2/ZnO thin film confirmed the E2 mode of ZnO. The appearance of three peaks, 395.6 cm^{-1}, 514.9 cm^{-1} and 629.7 cm^{-1}, confirmed the anatase TiO_2 phase, and the peak at 342.5 cm^{-1} confirmed the rutile TiO_2 in the TiO_2/ZnO. The presence of all corresponding ZnO and TiO_2 peaks in the Raman scattering indicate that the TiO2/ZnO thin-film substrates exist as a mixed crystalline structure of both materials.

(Received April 15, 2015; accepted May 7, 2015)

Keywords: TiO_2, ZnO, Raman, Photocatalysis, Composite films, Profilometry

1. Introduction

The present work aims to investigate the crystal quality, structural defects and disorders of mixed TiO2/ZnO and TiO_2/ZnO/TiO_2/ZnO oxide composite films fabricated using the sol-gel spin coating technique [1, 2]. It is well known that metal oxides are versatile materials commonly used in applications such as heterogeneous catalysts [3-5], gas sensors [6], light emitting diodes [7], antireflection coatings [8] and transparent electrodes in solar cells [9]. Thin films of metal oxides can be prepared using a variety of methods including the sol-gel spin coating route [10], vacuum arc plasma evaporation [11, 12], chemical vapor deposition (CVD) [13] and electrochemical methods [14-16]. Nevertheless the sol-gel spin coating route allows both for the convenient production [17] of thin films in any possible shape, but also for the preparation of porous materials whose pore-size distribution can be controlled both by the chemical composition of the starting material as well as the processing conditions.

In general TiO_2 and ZnO possess similar energy band gap values with both semiconductors finding different areas of application due to their physical and chemical properties. TiO_2 is an excellent choice photocatalyst [18, 19] due to its chemical stability, high quantum yield and non-toxicity or as a white pigment and optical reflective coating due to its high refraction index. On the other hand ZnO [20, 21] finds applications in optoelectronic devices [22-25] as a light emitter/detector or as a transparent conductive electrode due to its semiconductor large exciton binding energy, high transparency in the visible range and low electrical resistivity.

ZnO is less common in photocatalysis, nevertheless when used in composite films, particularly in combination with TiO_2, it can enhance the photocatalytic activity of the system [26-29]. It is well known that in photocatalytic applications TiO_2 is active under the UV range and a number of techniques such as suitable doping [30, 31] or addition of another metal-oxide semiconductor can enhance its photocatalytic activity in the visible range. Photocatalytic process is based on the generation of electron hole pairs by means of band-gap radiation that can give rise to redox reactions [32] with the species adsorbed on the surface of the photocatalysts. In principle the coupling of different semiconductor oxides [33] seems useful in order to absorb a wide range of solar radiation (both UV and visible regions) and to achieve a more efficient electron-hole pair separation and consequently a higher photocatalytic activity. Various composites-double layers- formed by TiO_2 and other oxides such as ZnO [34], SnO_2 [35] SiO_2 [36], CdS [37] Cu_2O [38], MgO [39], WO_3[40], MoO_3[41] etc. have been reported. Additionally it has been shown in literature that the semiconductor multilayers, such as ZnO/TiO_2/ZnO lead to improve the crystallinity of the ZnO fim by the TiO_2 buffer layer [42] as well as affecting the luminescence of ZnO. Additionally, the residual stress and the particle size of the ZnO thin film can be affected by the TiO_2 buffer layer. UV, green, yellow, and inconspicuous violet emissions were observed in PL measurements at room temperature. Nevertheless the preparation of such composite materials is always a challenge since the latter ones can combine the

advantages of each constituent, and moreover, the enhancement of preferred properties can be achieved in the composites.

The strongly interacting charge-spin and orbital ordering and the influence of the lattice in such materials yield unusual and useful properties [43] Thus the characterization of such composite materials requires a thorough investigation of their structure, which can be partially assessed using Raman spectroscopy [44, 45]. It is one of the excellent analytical techniques to investigate the crystallographic properties of thin film materials providing useful information on the existence of secondary phases with a submicron spatial resolution. Purity, phase-transition, lattice distortion and site occupancy are information that might be obtained under ambient or controlled atmosphere and temperature. Despite the fact that structural analysis of such thin films commonly employees X-ray diffraction, Raman spectroscopy poses advantages due to its ability to allow spectra to be collected from a very small volume, even below 1μm in diameter, which is simultaneously observed using a light microscope. Also, in Raman spectroscopy the amorphous phase does not contribute to a background of the spectrum [46], thus reducing the information noise and providing a detailed tool for examining crystal structures and stresses as well as indicating temperature chances in the investigated materials.

2. Materials and methods

The following chemicals were used in sample preparation: titanium (IV) oxide, mixture of rutile and anatase nanopowder <100nm particle size (BET) (99.5% trace metal basis Sigma Aldrich, Germany), zinc acetate dihydrate [Zn(CH3COO)2·2H2O](99%, Baker), absolute ethanol (Merck, Germany), diethyleneglycole (DEG, ReagentPlus 99%, Sigma Aldich), diethylamine (DEA, >99,5%, Sigma Aldich.

2.1. Preparation of TiO_2 /ZnO composite films

The TiO_2/ ZnO composite films were prepared on glass substrates by sol-gel spin coating technique. The glass substrates were cleaned with ethanol in an ultrasonic bath for 20 min and kept in a drying oven. A TiO_2 crystalline homogeneous paste was prepared using 0.4 g of TiO_2 nanopowder (<100nm particle size) with the addition of 5ml of ethanol and 10ml of diethyleneglycole (DEG) and stirred for 3 days at 60^o C. The procedure of preparing the ZnO layer involved 0.25M solution of zinc acetate dehydrate ($Zn(CH_3COO)_2{\cdot}2H_2O$) in ethanol under magnetic stirring for 20 minutes. After that 10 drops of diethylamine (DEA) were added as a stabilising agent and it was further stirred for 3 hours at 60^{o}C.

After that a first layer of TiO_2 was deposited under spin coating at 3000rpm for 1 minute. Then the films were dried at 100^{o}C for 5 minutes in order to evaporate the solvent and organic residues. The processes of spin coating and pre-heat treatment were repeated 10 times to obtain the desired thickness. Following that a first layer of ZnO was deposited in exactly the same fashion which was again repeated 10 times. Finally the films were annealed at 450^{o}C for 1 hour in air atmosphere.

2.2. Preparation of TiO_2/ZnO/ TiO_2/ZnO composite films

The TiO_2/ZnO/ TiO_2/ZnO composite films were prepared on glass substrates by sol-gel spin coating technique in exactly the same manner as the TiO_2/ ZnO layer composite films and finally annealed at 450^{o}C for 1 hour in air atmosphere.

3. Results and discussion

3.1. Characterization of TiO_2/ZnO and TiO_2/ZnO/TiO_2/ZnO composite films

3.1.1. Profilometer measurements

Surface studies of the composite films were made using an AMBIOS XP-2 stylus type profilometer. The layout of the profilometer is shown in Fig. 1 and the profile graph generated during the measurement of the thickness of samples 1, 2 and 3, can be seen in Figs. 2, 3 and 4 respectively. We have noted that in AMBIOS XP-2 stylus the step height repeatability is guaranteed to be 10Å or 0.1% of the nominal step value, whichever is greater.

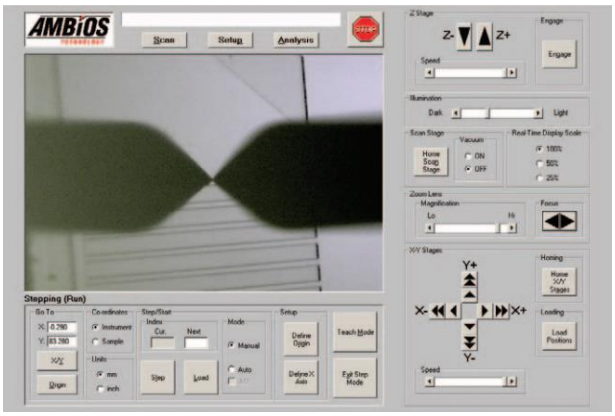

Fig. 1. The layout of the profilometer during the measurements.

Table 1. Sample Width measured using profilometer.

Sample	Layers	Total width (μm)	Material
1	2	3.2	TiO_2/ZnO
2	4	4.8	TiO_2/ZnO/ TiO_2/ZnO
3	4	5.2	TiO_2/ZnO/ TiO_2/ZnO

Figs. 2 to 4 of width profile of the three samples demonstrate the surface roughness of all the samples as a result of the fabrication using the sol gel technique. The total width of the samples was measured with an accuracy of 4-5% but we aim at a future stage to use an SEM technique in order to define the exact individual width of each layer as well as study the surface topology of the samples. Thus at this stage we present the average values of the measurements for the total width of the samples in μm which is given in Table 1.

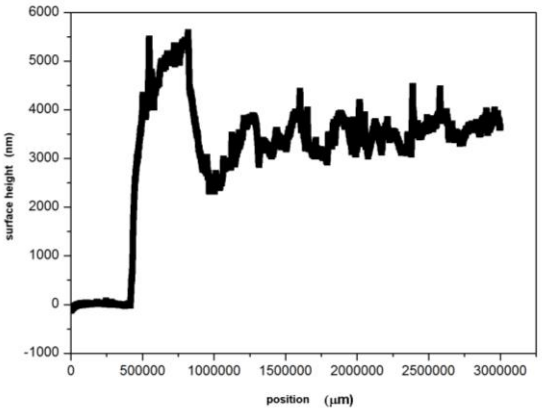

Fig. 2. The profile of the double layer of TiO_2/ZnO f ilm (Sample 1).

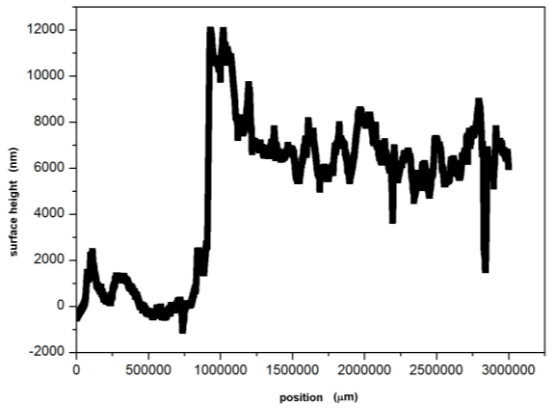

Fig. 3. The profile of the multilayer of TiO_2/ZnO/ TiO_2/ZnO film (Sample 2).

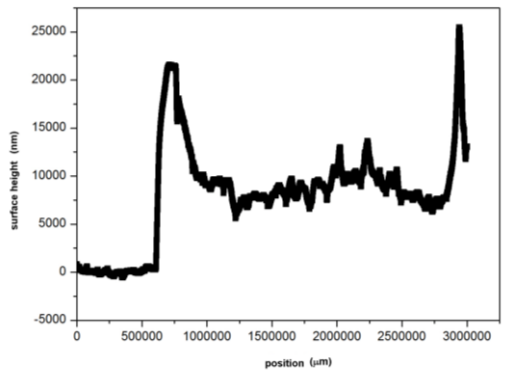

Fig. 4. The profile of the multilayer of TiO_2/ZnO/ TiO_2/ZnO film (Sample 3).

3.1.2 Raman spectroscopy experimental results

DeltaNU 785 nm portable Raman Spectrometer is used for the analysis. It is equipped with a class IIIB laser source that operates at 785 nm and from 50 to 120 mW. It has 35micron spot size of laser, resolution of 5cm^{-1} and spectral range 200-2000cm^{-1}. A digital microscope and a color video camera are used to define the best distance between substrate and the laser beam. The Raman Spectra of sample 1, 2 and 3 are depicted in fig 5, 6 and 7 respectively.

The chemical binding character of ZnO lies between covalent and ionic. Due to the large ionicity of the bonds between Zn and O atoms (about 0.62 on the Phillips scale), the two binding partners can be denoted as $Zn2^+$ and $O2^-$ ions, respectively. In ambient conditions, the thermodynamically stable phase of ZnO is the hexagonal wurtzite structure. Under stress or upon growth on cubic substrates, ZnO can also exhibit rock-salt structure or zinc-blende structure, respectively.

Additionally titanium dioxide is known to exist in three crystalline modifications: rutile (tetragonal), brookite (orthorhombic) and anatase (tetragonal).

We used the methods of Raman Spectroscopy which is proved to be particularly successful for identification of local surroundings and changes in molecular interactions and phase structure, being a powerful tool for understanding the processes of interactions between molecules and active centers located on the solid surface of TiO_2 and ZnO.

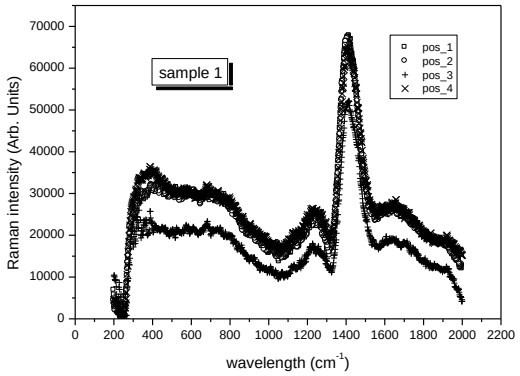

Fig. 5. Raman spectra of the of the double layer TiO_2/ZnO film (Sample 1).

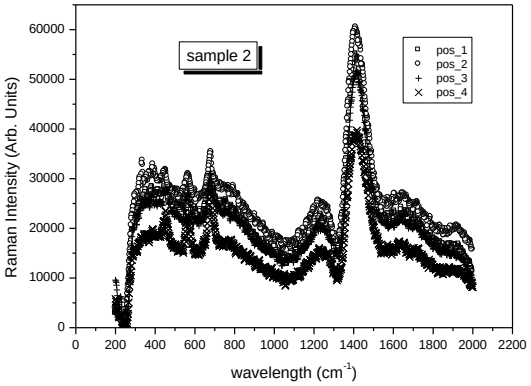

Fig. 6. Raman spectra of the multilayer TiO_2/ZnO/ TiO_2/ZnO film (Sample 2).

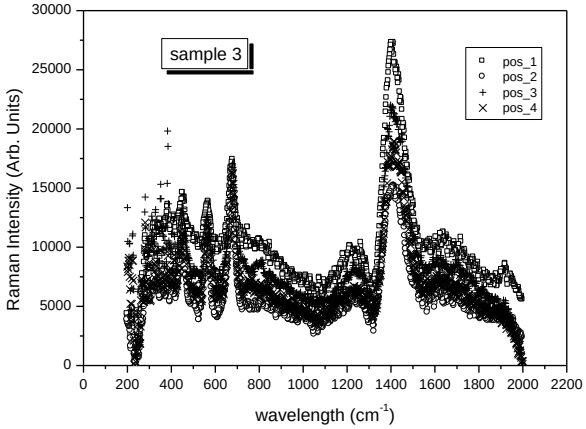

Fig. 7. Raman spectra of the multilayer TiO_2/ZnO/ TiO_2/ZnO film (Sample 3).

A sharp and strong peak at 436.9 cm^{-1} was observed in the ZnO and was assigned as the optical phonon E2 mode, which is a characteristic Raman-active peak for the wurtzite hexagonal phase of ZnO [47]. Two small peaks, 330 cm^{-1} and 377 cm^{-1} are also observed, and are attributed to be the E_{2H}-E_{2L} (multi phonon process) and the A_1T respectively. The presence of these in the spectrum is due to impurities and structural defects (oxygen vacancies and Zn interstitials) in the as-synthesized products. The TiO_2/ZnO substrate exhibited many peaks. The existence of the 436.9 cm^{-1} peak in the TiO_2/ZnO thin film confirmed the E2 mode of ZnO. The appearance of three peaks, 395.6 cm^{-1}, 514.9 cm^{-1} and 629.7 cm^{-1}, confirmed the anatase TiO_2 phase, and the peak at 342.5 cm^{-1} confirmed the rutile TiO_2 in the TiO_2/ZnO [48-50]. (Fig. 8-10).

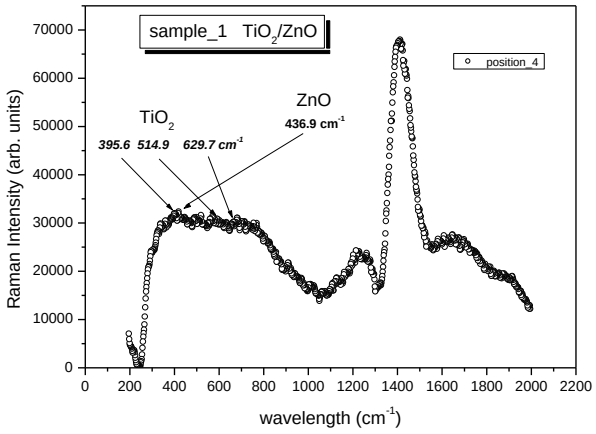

Fig. 8. Details of Raman spectra of the double layer TiO_2/ZnO film (Sample 1).

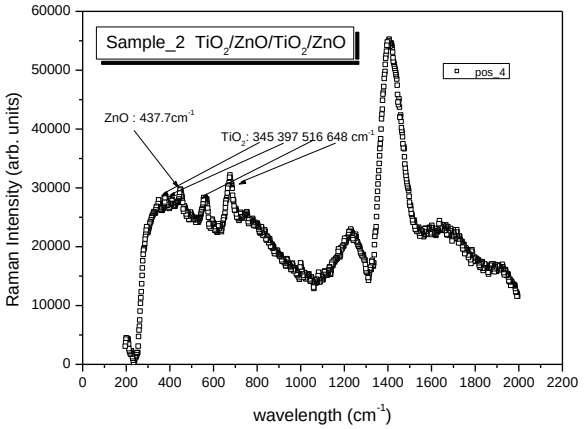

Fig. 9. Details of Raman of the multilayer TiO_2/ZnO/ TiO_2/ZnO film (Sample 2).

Thus, the presence of all corresponding ZnO and TiO_2 peaks in the Raman scattering indicate that the TiO_2/ZnO thin-film substrates exist as a mixed crystalline structure of both materials.

We anticipate from the above measurements that the above samples will possess low resistivity, nevertheless this needs to be further investigated using electric property measurements.

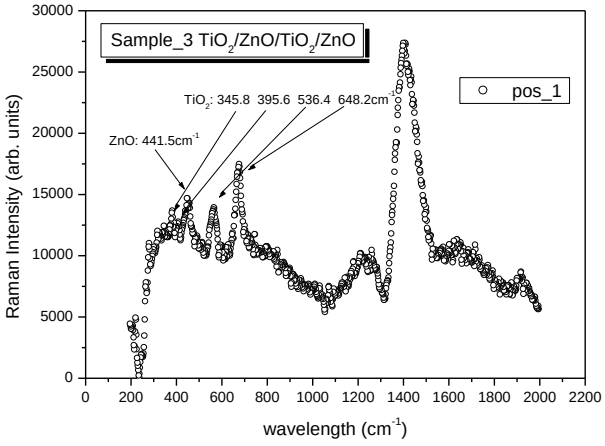

Fig. 10. Details of Raman of the multilayer TiO_2/ZnO/ TiO_2/ZnO film (Sample 3).

4. Conclusions

TiO_2/ZnO and TiO_2/ZnO/TiO_2/ZnO composite films were prepared by the sol-gel spin coating method. The prepared films were characterized using profilometry and Raman spectroscopy. The profilometry measurements indicate that the surfaces of the fabricated samples are not uniform. The total width of the samples was measured with an accuracy of 4-5% but we aim at a future stage to use an SEM technique in order to define the exact individual width of each layer as well as study the surface

topology of the samples. Additionally using Raman spectroscopy the presence of all corresponding ZnO and TiO_2 peaks in the Raman scattering indicate that the TiO2/ZnO thin-film substrates exist as a mixed crystalline structure of both materials. We anticipate from the above measurements that the above samples will possess low resistivity, nevertheless this needs to be further investigated using electric property measurements.

Acknowledgements

This research has been co-funded by the European Union (European Social Fund) and Greek national resources under the framework of the *Archimedes III: Funding of Research Groups in TEI of Athens* project of the Education and Lifelong Learning Operational Program.

The authors would like to thank Dr. Ioannis Raptis at Department of Microelectronics, Institute of Advanced Materials, Physicochemical Processes, Nanotechnology & Microsystems, NCSR 'Demokritos' for the use of the AMBIOS XP-2 stylus type profilometer.

References

[1] J. Tian, L. Chen, J. Dai, X. Wang, Y. Yin, P. Wu, Ceramics International **35** (6), 2261 (2009).
[2] D. L. Liao, C. A. Badour, B. Q. Liao, Journal of Photochemistry and Photobiology A, **194** (1), 11 (2008).
[3] J. Wang, J. Li, Y. Xie et al., Journal of Environmental Management, **91** (3), 677 (2010).
[4] Leda G. Bousiakou, Research Journal of Chemistry and Environment **19** (1) January (2015).
[5] Z. Zhang, Y. Yuan, Y. Fang, L. Liang, H. Ding, L. Jin, Talanta, **73**(3), 523 (2007).
[6] Q. Zhang, S. Zhang, C. Xie, C. Fan, Z. Bai, Sensors and Actuators B **128**, 586 (2008).
[7] D. C. Look, Mater Sci Eng. B **80**, 383 (2001).
[8] T. Ootsuka, Z. Liu, M. Osamura, Y. Fukuzawa, R. Kuroda, Y. Suzuki, N. Otogawa, T. Mise, S. Wang, Y. Hoshino, Y. Nakayama, H. Tanoue, Y. Makita, Thin Solid Films **476**, 30 (2005).
[9] O. Kluth, G. Schope, J. Hupkes, C. Agashe, J. Muller, B. Rech, Thin Solid Films **442**, 80 (2003).
[10] M. Wang, E. J. Kim, S. Kim, J. S. Chung, I. K. Yoo, E. W. Shin, S. H. Hahn, C. Park, Thin Solid Films **516**(6), 1124 (2008).
[11] T. Miyata, S. Tsukada, T. Minami, Thin Solid Films, **496**(1), 136 (2006).
[12] S. Wang, X. Wu, W. Qin, Z. Jiang, Electrochemical Acta **53**(4), 1883 (2007).
[13] C. E. Morosanu, Elsevier Science Publishing (1990).
[14] S. Bereznev, J. Kois, I. Golovtsov, A. Öpik, E. Mellikov, Thin Solid Films **425**, 511 (2006).
[15] O. Savadogo, Energy Materials and Solar Cells **52**(3), 361 (1998).
[16] N. Stratieva, E. Tzvetkova, M. Ganchev, K. Kochev, I. Tomov, Solar Energy Materials and Solar Cells **45**, 87 (1997)
[17] J. D. Wright, A. J. Nico, M. Sommerdijk, CRC Press (2001).
[18] K. Hashimoto, Japanese Journal of Applied Physics, **44**(12), 8269 (2005).
[19] M. Paleaz, N. Nolan, S. Pillai, ESHI Publications, Dublin Institute of Technology, ARROW@DIT (2012).
[20] S. S. Kumar et al, International Nano Letters **3**(30), (2013).
[21] Z. L. Wang, J. Phys. Condens. Matter **16**, R829 (2004).
[22] S. Y. Lee, E. S. Shim, H. S. Kang, S. S. Pang, Thin Solid Films **437**, 31 (2005).
[23] Z. L. Wang, X. Y. Kong, Y. Ding, P. Gao, W. L. Hughes, Adv. Funct. Mater **14**, 943 (2004).
[24] D. Brida, E. Fortunato, I. Ferreira, H. Aguas, R. Martins, J. Non-Cryst. Solids **299**, 1272 (2002).
[25] Z. L. Wang, J. Phys. Condens. Matter **16**, R829 (2004).
[26] Ge Ming, Guo Changsheng, Zhu Xingwang, Ma Lili, Han Zhenan, Hu Wei, Wang Yuqiu, Frontiers of Environmental Science & Engineering in China **3**(3), 271 (2003).
[27] W. Kostedt, A. A. Ismail, D. W. Mazyck, Ind Eng Chem Res **47**, 1483 (2008).
[28] S. F. Chen, W. Zhao, W. Liu, S. J. Zhang, Appl Surf Sci **255**, 2478 (2008).
[29] E. Evgenidou, K. Fytianos, I. Poulios, Appl Catal B: Environ **59**, 81 (2005).
[30] G. Colon, M. Maicu, M. C. Hidalgo, J. A. Navio, Applied Catalysis B, **67**(1-2), 41(2006).
[31] H. Yu, X. J. Li, S. J. Zheng, W. Xu, Materials Chemistry and Physics **97**(1), 59 (2006).
[32] M. Fox, M. T. Dulay, Chem. Rev. **93**(1), 341 (1993).
[33] C. Wang, B. Q. Xu, X. M. Wang, J. C. Zhao, Solid State Chem J. **178**, 3500 (2005).
[34] H. Bensouyad, D. Adnane, H. Dehdouh, B. Toubal, M. Brahimi, H. Sedrati, R. Bensaha, Sol-Gel Sci Technol J. **59**(3), 546 (2011).
[35] J. Yang, D. Li, X. Wang, X. J. Yang, L. D. Lu, J Solid State Chem, **165**, 193 (2002).
[36] C. Hu, Y. C. Tang, J. C. Yu, P. K. Wong, J photocatalyst Appl Catal B Environ. **40**, 131 (2003).
[37] L. Wu, J. C. Yu, X. Z. Fu, Mol Catal A Chem J. **244**, 25 (2006).
[38] J. L. Li, L. Liu, Y. Yu, Y. W. Tang, H. L. Li, F. P. Du, Electrochem Commun J. **6**, 940 (2004).
[39] J. Bandara C. C. Hadapangoda, W. G. Jayasekera, J Appl Catal B Environ **50**, 83 (2004).
[40] X. Z. Li, F. B. Li, C. L. Yang, W. K. Ge, Photochem Photobiol A Chem J. **141**, 209 (2001).
[41] Y. K. Takahashi, P. Ngaotrakanwiwat, T. Tatsuma, Electrochim Acta J. **49**, 2025 (2004).
[42] W. S. Choi et al, **83**, 878 (2009).
[43] N. Bahlawane, Raman Spectroscopy on Metal Oxide Thin Films (Application note) University of Bielefeld (February 2010).

[44] J. S. Tsang, The Jerusalem Symposia on Quantum Chemistry and Biochemistry **17**, 379 (1984).
[45] R. J. Nemanich, MRS Proceedings, **69** (1986).
[46] J. Ferraro, Second Edition Hardcover – Academic Press, (2002).
[47] D. F. Zhang, L. D. Sun, C. H. Yan, Chem. Phys. Lett., **422**(1-3), 46 (2006).
[48] X. J. Xing, Z. H. Xi, Z. Q. Xu, X. D. Zhang, J. H. Song, R. M. Wang, J. Xu, Y. Song, S. L. Zhang, D. P. Yu, Appl Phys Lett **83**, 1689 (2003).
[49] P. D. Yang, H. Q. Yan, S. Mao, R. Russo, J. Johnson, R. Saykally, N. Morris, J. Pham, R. R. He, H. J. Choi, Adv Funct Mater, **12**, 323 (2002).
[50] F. Q. He, Y. P. Zhao, J Phys D: Appl Phys **39**, 2105 (2006).

*Corresponding author: leda07@hotmail.com